Totally Adaptive Observer for Speed Sensorless Induction Motor Drives: Simply a Cost of Extra Energy Consumption

Jiahao Chen, Jin Huang, Ming Ye
College of Electrical Engineering, Zhejiang University, Hangzhou, China, horychen@zju.edu.cn

***Abstract*—This paper addresses the method for total parameters identification in speed sensorless induction motor drives. By total parameters identification, it means that all the inverse-Γ circuit parameters are poorly known and need to be identified. Based on the parameter sensitivity, an alternating-current (AC) signal of medium frequency (25 Hz) is superimposed onto the stator magnetizing current, so that the norms of columns of the regressive matrix of the voltage model are boosted, which rejects the disturbance of the unknown flux error and enforces convergence of the stator-side parameters. With stator-side parameters estimated, the remaining parameters are identified under the condition of persistent excitation. Effective simulation results are included.**

***Index Terms*—Parameter estimation, induction motor drives, speed sensorless control, parameter sensitivity analysis.**

I. Review on Multiple Parameters Identification in Alternating Current (AC) Drives

Parameter estimation of AC motors has been widely studied, as recently reviewed in [1], [2]. Nevertheless, the research on identification of both resistances and inductances in speed/position sensorless drives is not many in the literature. Generally, total parameters identification can be realized in drives with speed sensors [3], [4], but it is dismissed in the speed sensorless implementation [5]. Thus, the technical status of the multiple (not total) parameters identification in *sensorless* AC motor drives will be reported here.

A. Induction Motor (IM)

For induction motor, a back-stepping based observer that is adaptive to stator resistance, rotor resistance, magnetizing inductance and speed, has been designed by Rasmussen *et al.* [6], and to fulfill the persistency of excitation (PE) condition, a square wave is superimposed onto the magnetizing current. However, it is locally stable and is dependent on total leakage inductance.

On the other hand, a speed estimator that is immune to uncertainty in total leakage inductance is given by Zhen and Xu [7], and it is extended to further include stator and rotor resistances identification. However, it in turn requires the knowledge of magnetizing inductance (as well as that of rotor inertia).

This work was supported in part by the National Key Basic Research Program of China (973 Project) under Grant 2013CB035604 and in part by the National Natural Science Foundation of China under Grant 51690182.

Finally, a research on total parameter identification is conducted by Minami *et al.* [8], [9], where they devise three interconnected regression models for speed, stator resistance, and other electrical parameters, respectively. In their implementation, other parameters will converge only if the estimated value of the stator resistance is preset to a fixed value. The method can be interpreted as the subset selection [10], [11], and has been also applied to synchronous generator [12].

B. Surface-mounted Permanent Magnet Synchronous Motor

For surface-mounted permanent magnet synchronous motor (PMSM), an adaptive interconnected observer is proposed [13], where the interconnected rearrangement of the motor model yields two bilinear sub-systems. The results are: i) asymptotical convergence of estimation of stator resistance, stator inductance, load torque, rotor speed, and rotor position; ii) all the estimation errors are *practically stable* if exposed to uncertainty in rotor flux magnitude and other mechanical parameters. However, the *regular* PE condition of the inputs (to each sub-system) are not examined therein, so that the existence of the upper bounds of the time-varying gain matrices (denoted by S_1, S_2 and S_η in [13]) is not guaranteed. In effect, since the *regular* PE condition is expressed by the state transition matrix[1], it is difficult to be checked, as stated in Zhang [15].

Note that, in the above scheme, the identification of rotor flux magnitude is not considered. In fact, it is reported that simultaneous identification of stator resistance and rotor flux magnitude is not possible in normal operation of sensorless surface-mounted PMSM drives [16].

C. Interior PMSM

For interior PMSM, provided that rotor speed and rotor position are estimated from the extended electromotive force (EEMF) model, a stand-alone recursive least-square (RLS) based parameter identification of stator resistance and both d-axis and q-axis inductances is achieved by injecting pseudo random binary sequence onto both γ-axis and δ-axis current commands [17]. It should be noted that the parameter vector in

[1]The state transition matrix $\Phi_u(\tau, t)$ can be defined by [14]

$$\frac{d}{d\tau}\Phi_u(\tau,t) = A(u(\tau))\Phi_u(\tau,t), \quad \Phi_u(t,t) = \text{unit matrix},$$

where A is the homogeneous matrix, u the input, and τ, t the time instants.

978-1-5090-4281-4/17/$31.00 ©2017 IEEE

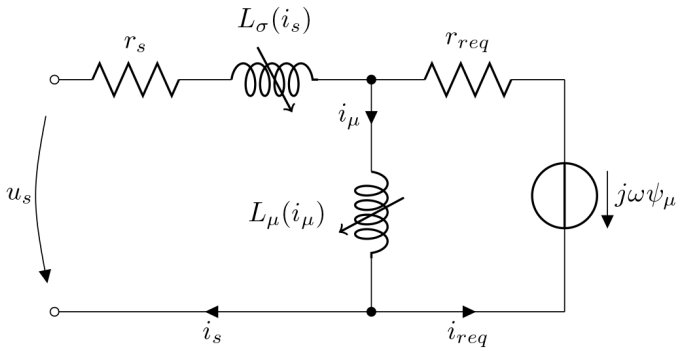

Fig. 1. Inverse-Γ circuit of induction motor [18].

the linear regression model is function of rotor speed error and rotor position error, so the parameter identification is only valid in steady state, and may be vulnerable to sudden load change. Besides, RLS does not account for noise and modelling error (e.g., rotor flux harmonics) in data matrix.

II. The Totally Adaptive Design for IMs

In this section, the total parameters identification in sensorless IM drives is presented, while the key, how the design works, heavily lies in the parameter sensitivity, and it will be elaborated in the following sections.

A. Mathematic Model of IM

The induction motor dynamics in the stationary α-β frame are described by the fifth-order equations (1)

$$L_\sigma p i_s = u_s - r_s i_s - p\psi_\mu \tag{1a}$$
$$p\psi_\mu = r_{req}\left(i_s - L_\mu^{-1}\psi_\mu\right) + \omega J \psi_\mu \tag{1b}$$
$$J_s n_{pp}^{-1} p\omega = n_{pp}\left(i_s^T J \psi_\mu\right) - T_L \tag{1c}$$

where $p = \frac{d}{dt}$ denotes differentiation operator, the inverse-Γ circuit parametrization is adopted (see Fig. 1):

- Stator-side parameters are stator resistance r_s and total leakage inductance L_σ. Stator-side signals are stator voltage $u_s = [u_{\alpha s}, u_{\beta s}]^T$ and stator current $i_s = [i_{\alpha s}, i_{\beta s}]^T$.
- Rotor-side parameters are equivalent rotor resistance r_{req} and equivalent magnetizing inductance L_μ. Rotor-side signals are equivalent rotor current i_{req} and equivalent rotor flux (linkage) $\psi_\mu = L_\mu(i_s + i_{req}) = L_\mu i_\mu$.
- Mechanical parameters are electrical rotor speed ω, load torque T_L, shaft inertia J_s, and number of pole pairs n_{pp}.

and $I = \begin{bmatrix} 1 & 0 \\ 0 & 1 \end{bmatrix}$, $J = \begin{bmatrix} 0 & -1 \\ 1 & 0 \end{bmatrix}$.

B. Two Reduced-order Flux Estimators

We extends the design in [19] to further include inductances identification. Thus, two flux estimators in stationary α-β frame are established respectively from (1a) and (1b)

$$p\hat{\psi}_\mu^{\mathrm{VM}} = u_s - \hat{r}_s i_s - \hat{L}_\sigma p i_s + v^{\mathrm{VM}} \tag{2a}$$
$$p\hat{\psi}_\mu^{\mathrm{CM}} = -\hat{\alpha}\left(\hat{\psi}_\mu^{\mathrm{CM}} - \hat{L}_\mu i_s\right) + \hat{\omega} J \hat{\psi}_\mu^{\mathrm{CM}} \tag{2b}$$

where superscripts $^{\mathrm{VM}}$ and $^{\mathrm{CM}}$ stand for voltage model and current model, respectively; a hat $\hat{}$ denotes estimated quantities, $\hat{\alpha} = \hat{r}_{req}\big/\hat{L}_\mu$ is the estimated reciprocal of the rotor time constant, and v^{VM} is the corrective term specified later. If $v^{\mathrm{VM}} = 0$, then (2) describes two open-loop flux estimators, of which (2a) is critically stable.

Next, define the flux mismatch ε and the flux error e,

$$\begin{aligned} \varepsilon &\triangleq \hat{\psi}_\mu^{\mathrm{VM}} - \hat{\psi}_\mu^{\mathrm{CM}} \\ e &\triangleq \psi_\mu - \hat{\psi}_\mu^{\mathrm{CM}} \end{aligned} \tag{3}$$

and the dynamics of ε and e follow as (4)

$$p\varepsilon = v^{\mathrm{VM}} + (\omega J - \alpha I)\, e + \Phi\tilde{\theta} \tag{4a}$$
$$pe = (\omega J - \alpha I)\, e + \Phi^{\mathrm{CM}}\tilde{\theta}^{\mathrm{CM}} \tag{4b}$$

with $\tilde{\theta} = [\tilde{\theta}^{\mathrm{VM}^T}, \tilde{\theta}^{\mathrm{CM}^T}]^T$ the parameter error vector and $\Phi = [\Phi^{\mathrm{VM}},\ \Phi^{\mathrm{CM}}]$ the regressive matrix, where

$$\begin{aligned} \tilde{\theta}^{\mathrm{VM}} &= \begin{bmatrix} \tilde{r}_s & \tilde{L}_\sigma \end{bmatrix}^T,\ \tilde{\theta}^{\mathrm{CM}} = \begin{bmatrix} \tilde{r}_{req} & \tilde{L}_\mu & \tilde{\omega} \end{bmatrix}^T, \\ \Phi^{\mathrm{VM}} &= \begin{bmatrix} i_s & p i_s \end{bmatrix}, \\ \Phi^{\mathrm{CM}} &= \begin{bmatrix} i_s - L_\mu^{-1}\hat{\psi}_\mu^{\mathrm{CM}} & \hat{\alpha} L_\mu^{-1}\hat{\psi}_\mu^{\mathrm{CM}} & J\hat{\psi}_\mu^{\mathrm{CM}} \end{bmatrix} \end{aligned}$$

and a tilde $\tilde{}$ designates the estimated error, e.g., $\tilde{\omega} = \omega - \hat{\omega}$.

To stabilize the critically stable dynamics of the mismatch ε, the corrective term is now determined by

$$v^{\mathrm{VM}} = -k^{\mathrm{VM}}\varepsilon, \quad k^{\mathrm{VM}} \in \mathbb{R}_+. \tag{5}$$

In other words, the output of the voltage model (2a) will now stay close to that of the stable current model (2b).

C. The Total Parameters Adaptation Rules

Both ε and e indicate parameter uncertainty, but only ε is available to update parameters. Hence, the parameter adaptation rules are devised as

$$p\begin{bmatrix} \hat{\theta}^{\mathrm{VM}} \\ \hat{\theta}^{\mathrm{CM}} \end{bmatrix} = \Gamma \begin{bmatrix} \Phi^{\mathrm{VM}^T} \\ \Phi^{\mathrm{CM}^T} \end{bmatrix} \varepsilon \tag{6}$$

where $\Gamma = \mathrm{diag}\,(\gamma_1, \gamma_2, \gamma_3, \gamma_4, \gamma_5)$, $\gamma_i \in \mathbb{R}_+, i = 1, 2, \ldots, 5$ is the diagonal gain matrix. Note that the current derivative pi_s in Φ^{VM} is not available, and in this paper, we simply use $p\hat{i}_s = \hat{L}_\sigma^{-1}\left(u_s - \hat{r}_s i_s - p\hat{\psi}_\mu^{\mathrm{CM}}\right)$ to replace pi_s and choose a small γ_2. Also, we replace L_μ in the first column of Φ^{CM} with $\hat{L}_\mu$, and replace L_μ in the second column of Φ^{CM} with 1.

In the sequel, we will refer to the persistency of excitation (PE) condition, meaning that for some interval $T \in \mathbb{R}_+$, the matrix (corresponding to θ^{VM} and θ^{CM})

$$\int_t^{t+T} \begin{bmatrix} \Phi^{\mathrm{VM}} & \Phi^{\mathrm{CM}} \end{bmatrix}^T \begin{bmatrix} \Phi^{\mathrm{VM}} & \Phi^{\mathrm{CM}} \end{bmatrix} dt$$

or the matrix (corresponding to r_s and L_μ)

$$\int_t^{t+T} \begin{bmatrix} i_s & \hat{\alpha} L_\mu^{-1}\hat{\psi}_\mu^{CM} \end{bmatrix}^T \begin{bmatrix} i_s & \hat{\alpha} L_\mu^{-1}\hat{\psi}_\mu^{CM} \end{bmatrix} dt$$

is bounded and positive definite.

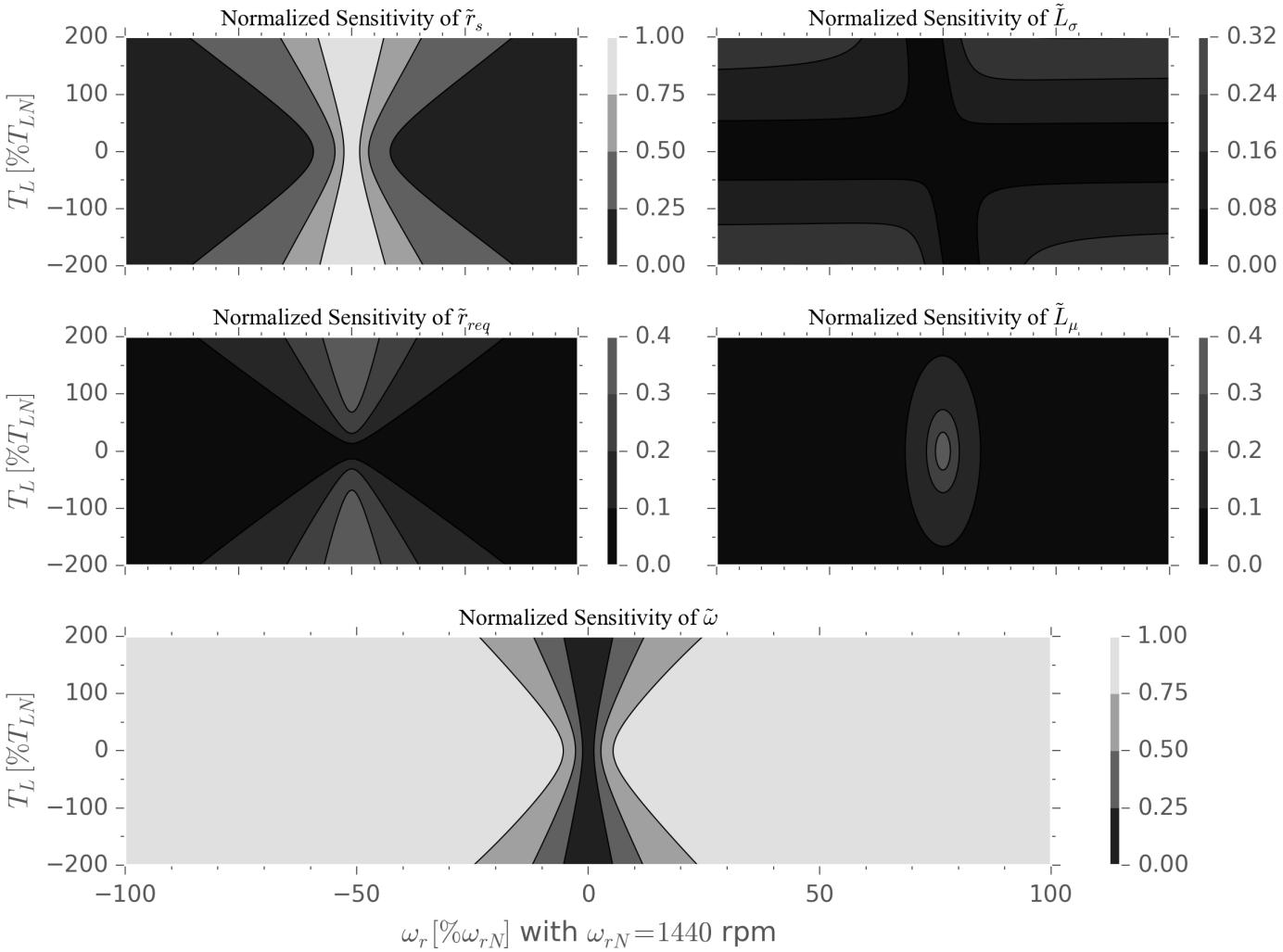

Fig. 2. Normalised sensitivity of parameter error over the working condition plane T_L-ω, i.e., the contour of the norm of each column of Φ_N. The flux modulus is fixed to 1.2 Wb. The motor data used is listed in the appendix.

III. Parameter Sensitivity Analysis

A. Parameter Sensitivity with respect to Working Conditions

During the parameter sensitivity analysis, the second-order error terms are neglected [20], so we have

$$\begin{aligned}\Phi^{\mathrm{VM}}\tilde{\theta}^{\mathrm{VM}} + \Phi^{\mathrm{CM}}\tilde{\theta}^{\mathrm{CM}} &\approx \Phi_N\tilde{\theta}_N \\ &\triangleq \begin{bmatrix} r_s i_s^T \\ L_\sigma p i_s^T \\ -r_{req} i_{req}^T \\ r_{req} i_\mu^T \\ \omega J \psi_\mu^T \end{bmatrix}^T \begin{bmatrix} \tilde{r}_s/r_s \\ \tilde{L}_\sigma \big/ L_\sigma \\ \tilde{r}_{req}/r_{req} \\ \tilde{L}_\mu \big/ L_\mu \\ \tilde{\omega}/\omega \end{bmatrix}\end{aligned} \tag{7}$$

where $i_\mu = \psi_\mu / L_\mu = i_s + i_{req}$ is the equivalent magnetizing current, $\tilde{\theta}_N$ the normalised parameter error vector, and Φ_N the first-order approximation of the regressive matrix corresponding to $\tilde{\theta}_N$. For each normalised parameter error, the norm of the corresponding column of Φ_N reflects the sensitivity of the very normalised parameter error with respect to changes in ε. To get an intuitive grasp of the parameter sensitivity, the norms of the five columns of Φ_N are plotted over different working conditions (i.e., load torque T_L and speed ω), as shown in Fig. 2. From Fig. 2, following statements are made:

1) At low speed, where the sensitivity of $\tilde{\omega}$ becomes comparable with that of $\tilde{L}_\mu$ and $\tilde{r}_{req}$, it is desired to identify L_μ and r_{req} along with r_s, so that speed estimation accuracy is improved. Note that to ensure the PE condition, usually sinusoids are superimposed onto the magnetizing current command i^*_{Ms}.
2) At high speed, only L_σ needs to be updated (if the load is sufficiently heavy). As a result, the requirement of flux modulus varying is relaxed. This is reasonable, because above the rated speed where stator voltage command u^*_s approaches voltage limitations of the inverter, flux modulus variation will impair motor torque capability.
3) Compared to the sensitivity analysis presented by Jadot *et al.* [20], one discovers that the sensitivity contours of $\tilde{r}_{req}$ and $\tilde{L}_\mu$ exhibit completely different functions to working conditions at very low speed. This is not due

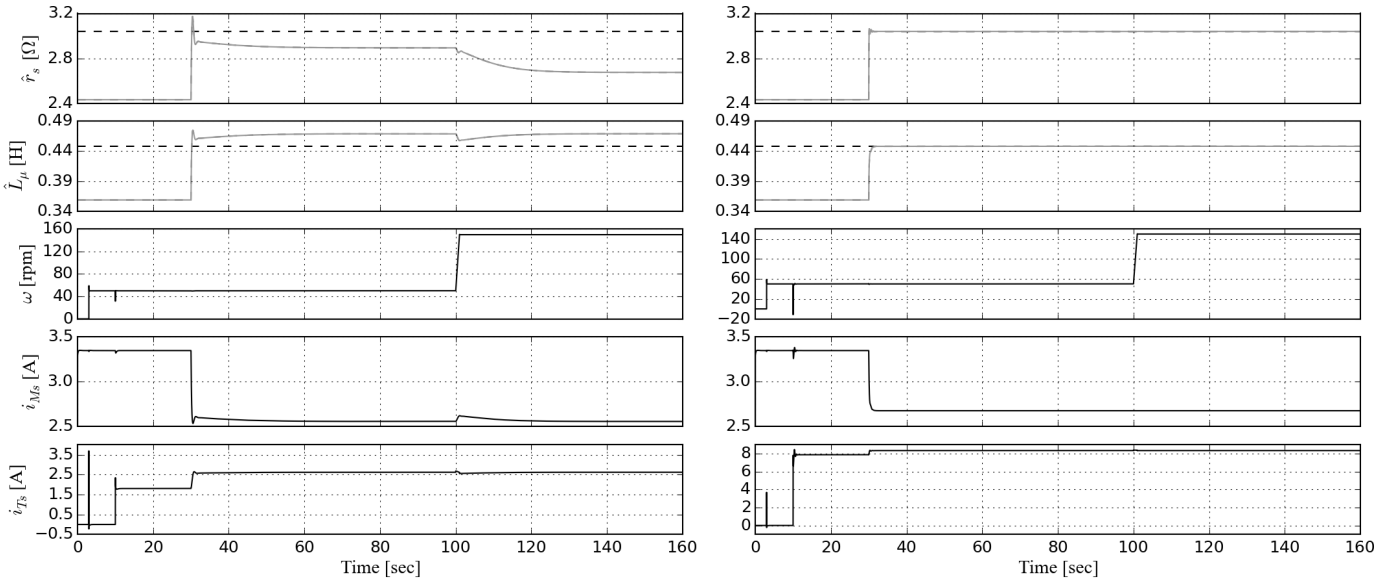

(a) T_L = 6 Nm (b) T_L = 20 Nm

Fig. 3. Simulated simultaneous identification of r_s and L_μ when sensed speed is used for control. Speed command is firstly $\omega^* = 50$ rpm and then goes up to $\omega^* = 150$ rpm. Load applied at 10 sec and adaptation begins at 30 sec. (a) biased estimation at light load. (b) consistent estimation at heavy load.

to the inclusion of the speed uncertainty, but is because of the different indicators for parameter uncertainty.

IV. Disturbance Rejection

The dynamics of the parameter errors are derived as

$$\begin{aligned} p\tilde{\theta} &= -\Gamma\Phi\varepsilon \\ &= -\Gamma\Phi\frac{\Phi\tilde{\theta}}{p+k^{\mathrm{VM}}} - \Gamma\Phi\frac{(\omega J-\alpha I)\,e}{p+k^{\mathrm{VM}}} \end{aligned} \tag{8}$$

Let us take a look at the homogeneous part of (8)

$$p\tilde{\theta} = -\Gamma\Phi^T\frac{\Phi\tilde{\theta}}{p+k^{\mathrm{VM}}} \tag{9}$$

which can be shown to be exponentially stable under the PE condition by applying [21, Theorem 2.3]. However, $\tilde{\theta}$ is disturbed by the unknown flux error e, and the asymptotical stability of $\tilde{\theta}$ is lost. In other words, once we adopt the flux estimators given in (2), we choose to bear with the theoretical disturbance e in the dynamics of ε. In this case, the PE condition is not anymore a sufficient condition for parameter convergence, but for merely bounded parameter estimation (indeed, the parameter error can become quite large) [22].

Intuitively, the gain of the 'disturbance channel' should be lowered, e.g., via an observer pole assignment by Tomita *et al.* [23]. However, the observer pole assignment affects not only the flux error e, but also the parameter sensitivity, so it is not considered as a good option.

Before we proceed to elucidate how to deal with the disturbance, it is rewarding to point out the fact that if $\tilde{\theta}^{\mathrm{VM}} = 0$, the dynamics of ε and e become in a form to which a Lyapunov function can be found and the Kalman-Yakubovich lemma can be applied [19], so ε and e are asymptotically stable and $\tilde{\theta}^{\mathrm{CM}}$ will converge to zero provided that the PE condition suffices.

A. Disturbance Reduction

From (4b), we notice that e depends on $\tilde{\theta}^{\mathrm{CM}}\Phi^{\mathrm{CM}}$. So, we rewrite (4) into the following form

$$\begin{aligned} \varepsilon &= \tfrac{\Phi\tilde{\theta}}{p+k^{\mathrm{VM}}} + \tfrac{(\omega J-\alpha I)e}{p+k^{\mathrm{VM}}} \\ &= \tfrac{\Phi\tilde{\theta}}{p+k^{\mathrm{VM}}} + \tfrac{(\omega J-\alpha I)[pI-(\omega J-\alpha I)]^{-1}\Phi^{\mathrm{CM}}\tilde{\theta}^{\mathrm{CM}}}{p+k^{\mathrm{VM}}} \end{aligned} \tag{10}$$

This implies that if the motor operates in a working condition where the sensitivity of $\tilde{\theta}^{\mathrm{CM}}$ is low while the sensitivity of $\tilde{\theta}^{\mathrm{VM}}$ is high, then $\tilde{\theta}^{\mathrm{VM}}$ will tend towards zero until the norm of $\Phi^{\mathrm{VM}}\tilde{\theta}^{\mathrm{VM}}$ becomes comparable to that of $\Phi^{\mathrm{CM}}\tilde{\theta}^{\mathrm{CM}}$. Besides, if $\tilde{\theta}^{\mathrm{VM}}$ is sufficiently close to zero, then $\tilde{\theta}^{\mathrm{CM}}$ converges towards zero under the PE condition. To make sense of the above statement, we conduct the following simulation based on (2) and (6). (See appendix for the numeric values used in the simulation and the definitions of i_{Ms} and i_{Ts}.)

1) Identification of r_s and L_μ for illustrating the influence of the disturbance e: In Fig. 3, the simulation results of the simultaneous identification of r_s and L_μ at low speed are presented. Note that the PE condition in this case is always satisfied as long as the load torque is nonzero. In Fig. 3(a), where the load is light so that the sensitivity of $\tilde{L}_\mu$ is high, the rotor-side parameter error $\tilde{L}_\mu$ causes large e, and large e further leads to biased estimation of $\hat{r}_s$ and $\hat{L}_\mu$, even when the PE condition (i.e., $T_L \neq 0$) is satisfied. While in Fig. 3(b), where the load is heavy so that the sensitivity of $\tilde{L}_\mu$ becomes low, it is observed that r_s and L_μ are consistently estimated, because the disturbance e is notably reduced.

In conclusion, in the working conditions where e is insignificant, consistent estimation of parameters is possible, while in some other working conditions where e is noteworthy, though the PE condition cannot assure the convergency of parameters estimation, it is still crucial for system stability.

B. Parameter Sensitivity Shaping

The disturbance reduction discussed above relies on the working conditions that are usually not at our disposal, so it is of merely theoretical interest and infeasible. Rather, our objective is then altered to raise the 'signal-to-noise ratio' in a proactive manner, that is, by increasing the stator-side parameter sensitivity, the influence of the disturbance e is relatively decreased. This idea is named parameter sensitivity shaping.

Specifically, since on the one hand, the sensitivity of the stator-side parameter errors $\tilde{\theta}^{\mathrm{VM}}$ is closely related to the norms of columns of Φ^{VM}, and on the other hand, the norm of the disturbance e depends on $\Phi^{\mathrm{CM}}\tilde{\theta}^{\mathrm{CM}}$, we should adjust the stator currents in a way in which the norms of columns of Φ^{VM} are boosted and in the meanwhile the norm of $\Phi^{\mathrm{CM}}\tilde{\theta}^{\mathrm{CM}}$ is not increased a lot. To this end, consider the flux modulus command with low-amplitude medium-frequency pulsation:

$$|\psi_\mu^*| = 1.2 + 0.01\sin(50\pi t) \quad (\mathrm{Wb}), \quad t \in \mathbb{R}_+ \tag{11}$$

In several papers that deal with simultaneous identification of rotor resistance and speed from the IM model, it is believed that it is the time-varying flux modulus that satisfies the PE condition (e.g., sinusoidal $\frac{d}{dt}|\psi_\mu|$ in [24] and constant $\frac{d}{dt}|\psi_\mu|$ in [19]). However, the selection of the frequency of the time-varying flux modulus is seldom discussed, except in [25], [26] (where it is suggested that the pulsating frequency of the flux modulus should be different from the synchronous speed). Here in this paper, it is shown how a medium-frequency component in the flux modulus is of benefit to disturbance rejection and as well to the PE condition fulfilment.

Two direct advantages of such a choice of flux modulus command follow. For one thing, the varying range of the saturation level is restricted (because $|\psi_\mu^*|$ varies between 1.19 and 1.21 Wb), so that the actual value of L_μ can still be assumed as a constant one. As a comparison, in the implementation of Kubota *et al.* [24], the variation of the saturation level caused by the *low-frequency* component in the magnetizing current needs to be compensated by the magnetizing curve obtained from the no-load test. For another, the torque ripple caused by the flux modulus pulsating is very limited. As a result, the cost of the total parameters estimation is the extra Joule loss owing to the large amplitude of the AC component in the commanded magnetizing current i_{Ms}^*

$$\begin{aligned} i_{Ms}^* &= \hat{r}_{req}^{-1} p\left|\psi_\mu^*\right| + \hat{L}_\mu^{-1}\left|\psi_\mu^*\right| \\ &= \tfrac{0.01\times 50\pi}{\hat{r}_{req}}\cos(50\pi t) + \tfrac{1}{\hat{L}_\mu}\left(1.2 + 0.01\sin(50\pi t)\right) \end{aligned} \tag{12}$$

In other words, we can increase the sensitivity of $\tilde{\theta}^{\mathrm{VM}}$ while keep the norm of $\Phi^{\mathrm{CM}}\tilde{\theta}^{\mathrm{CM}}$ not increase a lot, by injecting a medium-frequency AC signal (rather than a low-frequency one) onto the magnetizing current i_{Ms}. This assures the convergence of $\hat{\theta}^{\mathrm{VM}}$ even when exposed to e at low speed and light load, where the sensitivity of $\tilde{L}_\mu$ becomes remarkable. After $\tilde{\theta}^{\mathrm{VM}}$ arrives around zero, the asymptotical stability of ε, e, and $\tilde{\theta}^{\mathrm{CM}}$ is guaranteed by the PE condition. To validate the effectiveness of the idea of parameter sensitivity shaping, a simulation study based on (2) and (6) follows.

1) Low speed operation with total parameters adaptation: In Fig. 4, presented are the simulation results of the total adaptation of r_s, L_σ, r_{req}, L_μ and ω with the flux modulus command $|\psi_\mu^*|$ given in (11). Before $t = 30$ sec, the motor speed ω experiences violent oscillations and its mean value is different from the speed command, because all the inverse-Γ circuit parameters are poorly known. Particularly, i_{Ts} also oscillates and stays negative when T_L is null, and it becomes positive when T_L is applied. After $t = 30$ sec, the system is quickly stabilized with the total parameters adaptation. At $t = 100$ sec, the speed command goes up to 150 rpm with the total adaptation turned on, and no estimation deviation (especially of r_{req}) occurs during the speed transient. As a comparison, in the implementation of [26, Figure 9.5], the r_{req} estimation undergoes drastic deviation in speed transient, to which the counter-measures are fortunately available, e.g., via the speed independent adaptation rule [27] or the hybrid algorithm [19].

Therefore, the effectiveness of the idea of parameter sensitivity shaping has been validated for both steady state and transient operations. Further observations from Fig. 4 are listed:

1) It is observed that, thanks to the low-amplitude flux modulus variation, the speed distortion is found very limited after parameters converge.
2) We notice that r_s and r_{req} are slightly bias estimated. This is due to the fact that the sensitivity of $\tilde{r}_{req}$ is also increased since the medium-frequency component of the stator current will also flow through the branch of the rotor that is less resistant/reluctant than the branch of the magnetization (refer to Fig. 1).
3) Generally speaking, in speed-sensorless drives, a slow adaptation would enhance the robustness of the whole contorl system. Specifically, for resistances, the adaptation can be made slow owing to the slow variation of temperature; while for L_μ, faster adaptation is preferred for the saturation level may vary fast. On account of this fact, a large γ_4 should be considered when the sensitivity of $\tilde{L}_\mu$ diminishes. As shown in Fig. 4, the adaptation of L_μ does response promptly and it gets into oscillation. Such oscillation is caused by the large detuned resistances. In practice, large uncertainty in resistances is not likely to arise, since the variation of resistances is always compensated by the slow resistances adaptation.
4) Unlike i_{Ts}, the stator magnetizing current i_{Ms} consists of a DC bias as well as a large amplitude of AC component, which contributes to the side effect of the parameter sensitivity shaping, i.e., the extra energy consumption.

V. Conclusion

We have presented a totally adaptive design that actualizes the simultaneous adaptivity to r_s, L_σ, r_{req}, L_μ, and ω, which works stably even during speed transient. Based on

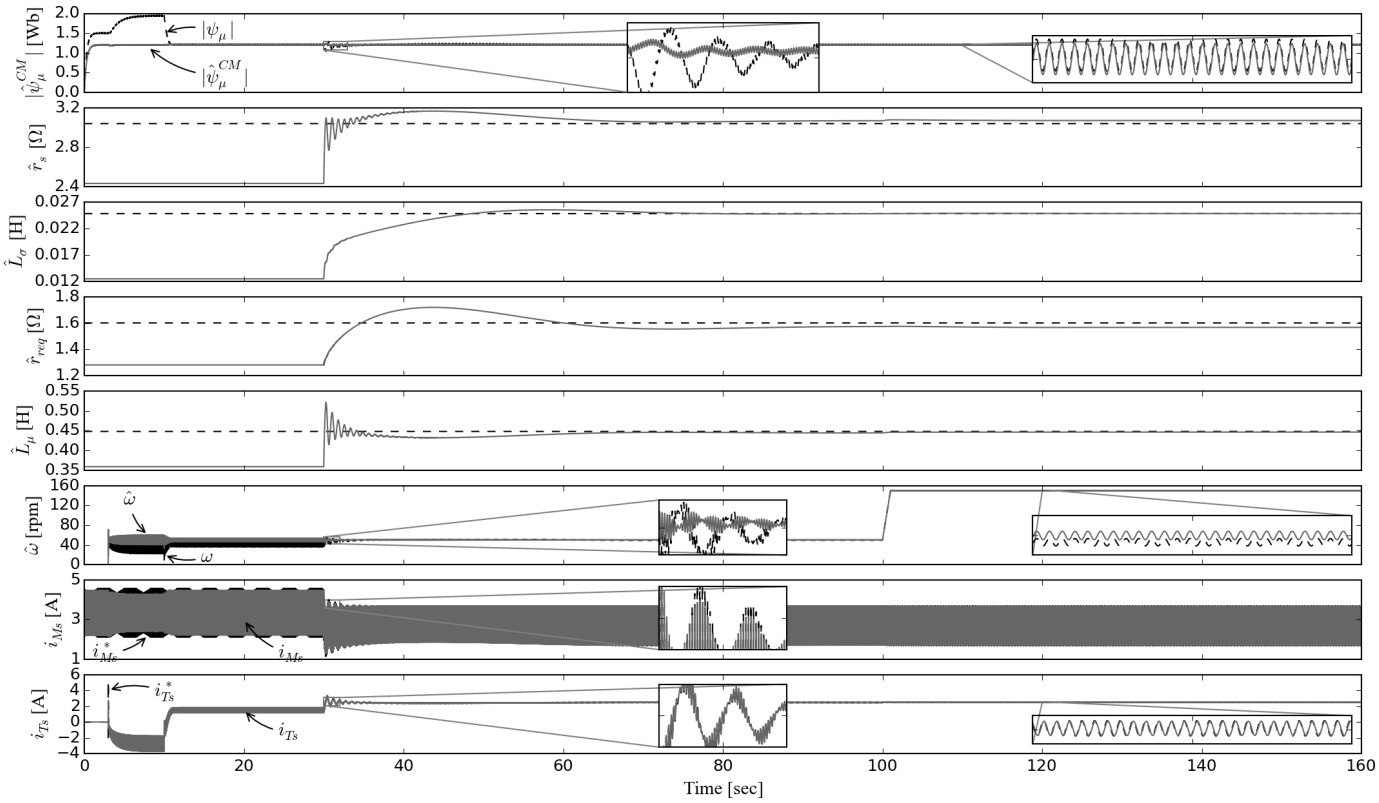

Fig. 4. Simulated total parameters adaptation in speed sensorless IM drive with the flux modulus command given in (11). Except that of speed, adaptation of r_s, L_σ, r_{req} and L_μ begins at $t = 30$ sec. Load torque is applied at $t = 10$ sec. Speed command is firstly 50 rpm and then goes up to 150 rpm.

the simulation studies, we have managed to show how a low-amplitude medium-frequency component in the flux modulus is beneficial to disturbance rejection, to lower speed distortion, and to the PE condition fulfilment. Such excitation stems from the idea of parameter sensitivity shaping. It is a disturbance rejection technique via the adjustment of the regressive matrices that are closely related to the parameter sensitivity. The PE condition is also found achieved by injecting stator currents of distinct frequencies, rather than by fluctuating the flux modulus. Therefore, speed ripples are insignificant because the pulsating of the flux modulus is limited. As a result, the total parameters identification is realized at a cost of extra energy consumption (such as copper loss and iron loss) that is due to the AC component in the stator magnetizing current.

In addition, from the parameter sensitivity analysis, it is suggested that the extra excitation may be dismissed when motor speed is high. The study is still primitive, where we have to assume there is no skin effect, and L_σ is constant.

APPENDIX

NUMERIC DATA AND SUPPLEMENTARY SPECIFICATION

Numeric values of the inverse-Γ circuit parameters are $r_s = 3.04\ \Omega$, $r_{req} = 1.60\ \Omega$, $L_\sigma = 0.0249$ H, and $L_\mu = 0.448$ H.

The control strategy adopted in this paper is the indirect field orientated control (the same with that of [19]). The field oriented frame is established in the controller, with M-axis aligned along the rotor flux vector and T-axis 90° leading to the M-axis, and the definitions of the stator magnetizing current i_{Ms} and the stator torque current i_{Ts} are now clear.

In Fig. 3, numeric values of the observation and adaptation coefficients are $k^{\mathrm{VM}} = 100$, $\Gamma = \mathrm{diag}(25, 0, 0, 15, 0)$, and particularly we put $\hat{\omega} = \omega$.

In Fig. 4, speed sensorless control is implemented, and we have $k^{\mathrm{VM}} = 100$, and $\Gamma = \mathrm{diag}(25, 0.1, 25, 15, 6e5)$.

REFERENCES

[1] C. Verrelli, A. Savoia, M. Mengoni, R. Marino, P. Tomei, and L. Zarri, "On-line identification of winding resistances and load torque in induction machines," *Control Systems Technology, IEEE Transactions on*, vol. 22, no. 4, pp. 1629–1637, July 2014.

[2] S. A. Odhano, R. Bojoi, M. Popescu, and A. Tenconi, "Parameter identification and self-commissioning of ac permanent magnet machines - a review," in *Electrical Machines Design, Control and Diagnosis (WEMDCD), 2015 IEEE Workshop on*, March 2015, pp. 195–203.

[3] M. Cirrincione, M. Pucci, G. Cirrincione, and G. A. Capolino, "A new experimental application of least-squares techniques for the estimation of the induction motor parameters," *IEEE Transactions on Industry Applications*, vol. 39, no. 5, pp. 1247–1256, Sept 2003.

[4] ——, "Constrained minimization for parameter estimation of induction motors in saturated and unsaturated conditions," *IEEE Transactions on Industrial Electronics*, vol. 52, no. 5, pp. 1391–1402, Oct 2005.

[5] ——, "Sensorless control of induction motors by reduced order observer with mca exin + based adaptive speed estimation," *IEEE Transactions on Industrial Electronics*, vol. 54, no. 1, pp. 150–166, Feb 2007.

[6] H. Rasmussen, P. Vadstrup, and H. Borsting, "Full adaptive backstepping design of a speed sensorless field oriented controller for an induction motor," in *Industry Applications Conference, 2001. Thirty-Sixth IAS Annual Meeting. Conference Record of the 2001 IEEE*, vol. 4, Sept 2001, pp. 2601–2606 vol.4.

[7] L. Zhen and L. Xu, "Sensorless field orientation control of induction machines based on a mutual mras scheme," *IEEE Transactions on Industrial Electronics*, vol. 45, no. 5, pp. 824–831, 1998.
[8] K. Minami, M. Velez-Reyes, D. Elten, G. C. Verghese, and D. Filbert, "Multi-stage speed and parameter estimation for induction machines," in *Power Electronics Specialists Conference, 1991. PESC '91 Record., 22nd Annual IEEE*, Jun 1991, pp. 596–604.
[9] K. Minami, "Model-based speed and parameter tracking for induction machines," Master's thesis, Massachusetts Institute of Technology, 1989.
[10] M. Velez-Reyes and G. C. Verghese, "Subset selection in identification, and application to speed and parameter estimation for induction machines," in *Control Applications, 1995., Proceedings of the 4th IEEE Conference on*, Sep 1995, pp. 991–997.
[11] M. Velez-Reyes and R. Castro-Anaya, "Sensitivity and conditioning issues in speed sensorless control of induction motors," in *Industry Applications Conference, 1998. Thirty-Third IAS Annual Meeting. The 1998 IEEE*, vol. 1, Oct 1998, pp. 640–647 vol.1.
[12] M. Burth, G. C. Verghese, and M. Velez-Reyes, "Subset selection for improved parameter estimation in on-line identification of a synchronous generator," *IEEE Transactions on Power Systems*, vol. 14, no. 1, pp. 218–225, Feb 1999.
[13] M. A. Hamida, J. D. Leon, A. Glumineau, and R. Boisliveau, "An adaptive interconnected observer for sensorless control of pm synchronous motors with online parameter identification," *IEEE Transactions on Industrial Electronics*, vol. 60, no. 2, pp. 739–748, Feb 2013.
[14] G. Besançon, *Nonlinear observers and applications*. Berlin: springer, 2007, vol. 363.
[15] Q. Zhang, "Adaptive observer for multiple-input-multiple-output (mimo) linear time-varying systems," *IEEE Transactions on Automatic Control*, vol. 47, no. 3, pp. 525–529, Mar 2002.
[16] M. Rashed, P. F. A. MacConnell, A. F. Stronach, and P. Acarnley, "Sensorless indirect-rotor-field-orientation speed control of a permanent-magnet synchronous motor with stator-resistance estimation," *IEEE Transactions on Industrial Electronics*, vol. 54, no. 3, pp. 1664–1675, June 2007.
[17] S. Ichikawa, M. Tomita, S. Doki, and S. Okuma, "Sensorless control of permanent-magnet synchronous motors using online parameter identification based on system identification theory," *IEEE Transactions on Industrial Electronics*, vol. 53, no. 2, pp. 363–372, April 2006.
[18] G. R. Slemon, "Modelling of induction machines for electric drives," *IEEE Transactions on Industry Applications*, vol. 25, no. 6, pp. 1126–1131, Nov 1989.
[19] J. Chen and J. Huang, "Online decoupled stator and rotor resistances adaptation for speed sensorless induction motor drives by a time-division approach," *IEEE Transactions on Power Electronics*, vol. 32, no. 6, pp. 4587–4599, June 2017.
[20] F. Jadot, F. Malrait, J. Moreno-Valenzuela, and R. Sepulchre, "Adaptive regulation of vector-controlled induction motors," *Control Systems Technology, IEEE Transactions on*, vol. 17, no. 3, pp. 646–657, 2009.
[21] B. D. Anderson, R. R. Bitmead, C. R. J. Johnson, P. V. Kokotovic, R. L. Kosut, I. M. Mareels, L. Praly, and B. D. Riedle, *Stability of Adaptive Systems: Passivity and Averaging Analysis*. Cambridge, MA: MIT Press, 1986.
[22] R. Marino, G. L. Santosuosso, and P. Tomei, "Robust adaptive observers for nonlinear systems with bounded disturbances," *Automatic Control, IEEE Transactions on*, vol. 46, no. 6, pp. 967–972, 2001.
[23] M. Tomita, T. Senjyu, S. Doki, and S. Okuma, "New sensorless control for brushless dc motors using disturbance observers and adaptive velocity estimations," *IEEE Transactions on Industrial Electronics*, vol. 45, no. 2, pp. 274–282, Apr 1998.
[24] H. Kubota, D. Yoshihara, and K. Matsuse, "Rotor resistance adaptation for sensorless vector-controlled induction machines," *Electrical Engineering in Japan*, vol. 125, no. 2, pp. 65–72, 1998.
[25] I.-J. Ha and S.-H. Lee, "An online identification method for both stator- and rotor resistances of induction motors without rotational transducers," *IEEE Transactions on Industrial Electronics*, vol. 47, no. 4, pp. 842–853, Aug 2000.
[26] R. Marino, T. Patrizio, and M. C. Verrelli, "Adaptive output feedback control of induction motors," in *AC Electric Motors Control: Advanced Design Techniques and Applications*. Wiley Online Library, 2013, pp. 158–187.
[27] K. Kubota and K. Matsuse, "Speed sensorless field-oriented control of induction motor with rotor resistance adaptation," *Industry Applications, IEEE Transactions on*, vol. 30, no. 5, pp. 1219–1224, Sep 1994.